

NEW APPROACH OF ORBIT DETERMINATION STRATEGY TO IMPROVE THE STARDUST DYNAMIC MODELS¹

Tung Han You², Jordan Ellis³ & Tim McElrath⁴

Since the launch of Stardust in February 1999, the navigation team has encountered considerable difficulty in determining and predicting a consistent estimate of the Stardust orbit. The primary factors contributing to the estimation errors are the mismodelling of nongravitational accelerations due to both the solar radiation pressure and the small ΔV 's (referred to as small forces) that arise owing to the attitude control system. This paper describes the estimation strategy used to model the small forces, developed as a result of extensive analyses at Jet Propulsion Laboratory and Lockheed Martin Astronautics. The detailed spacecraft dynamic models and the evaluation of the dynamic error sources are discussed. A unique filter method has been developed to create a simple and efficient orbit determination strategy. Not only is it specifically designed to deal with Stardust's dynamic mismodelling but the estimation knowledge also can be used to optimize the orbit propagation models.

INTRODUCTION

Stardust is the first mission that will swing close to a comet (Wild 2) and return the collected cometary material and interstellar dust back to Earth for scientific research. Accurate navigation is vital for successful mission operations as well as science data return.

Since the launch of Stardust in February 1999, the navigation team has encountered considerable difficulty in determining and predicting a consistent estimate of the Stardust orbit. The primary factors contributing to the estimation errors are the mismodelling of nongravitational accelerations due to both the solar radiation pressure and the small ΔV 's that arise owing to the attitude control system (ACS).

This paper describes the estimation strategy used to model the small forces, developed as a result of extensive analyses at Jet Propulsion Laboratory (JPL) and Lockheed Martin Astronautics (LMA). The detailed spacecraft (S/C) dynamic models and the evaluation of

¹This work was carried out at the Jet Propulsion Laboratory, California Institute of Technology, Pasadena, California under contract to National Aeronautics and Space Administration

²Member of Technical Staff

³Multi-Mission Navigation Group Supervisor

⁴Mission Management Office Guidance, Navigation & Control Team Chief

the dynamic error sources are discussed. A unique filter method has been developed to create a simple and efficient orbit determination (OD) strategy. Not only is it specifically designed to deal with Stardust's dynamic mismodelling but the estimation knowledge also can be used to optimize the orbit propagation models. This filtering strategy decomposes the limit duty cycle into deadband walk, Earth-pointing, and Sun-pointing phases and constructs a characteristic stochastic batch size and level of process noise for each phase. The filter estimates the solar pressure coefficients and stochastic small force scale factors. The scale factor estimates in turn are used as a basis for predicting the effects of small forces for orbit propagation.

SPACECRAFT DYNAMIC MODELS

JPL's Double Precision Orbit Determination Program (DPODP) (Ref. 1, 2) is used to model spacecraft dynamics and observations. The trajectory is expressed in the J2000 Solar System Barycentric Reference frame. JPL Ephemeris DE405 is the source of planetary masses and ephemeris.

The primary factor contributing to the orbit propagation errors for Stardust is the mismodelling of nongravitational accelerations. Solar radiation pressure and small forces (SMF) are the two dominant nongravitational forces.

Solar Radiation

To model the nongravitational acceleration due to solar pressure, the Stardust spacecraft is decomposed into four component areas. Figure 1 shows the Stardust spacecraft structure. The components are defined in an orthogonal spacecraft fixed coordinate system with the solar panel normal along the S/C Z axis and the whipple shield on the launch vehicle adapter (mounted on central bus) normal along the S/C X axis. S/C Y axis is determined by $Z \times X$. The four areas include one two-sided flat plate to represent the solar panels and three two-sided flat plates to model the central bus (including the whipple shields mounted on the solar arrays).

The areas of the central bus and whipple shields are summed along the X, Y, and Z axes and one two-sided flat plate is assigned along each axis (X, Y, and Z plate). The solar radiation coefficients for the X, Y, and Z plates are average values.

The total solar radiation force, F_{solar} , experienced by the spacecraft is expressed as

$$F_{solar} = \left(\frac{C_{sf} K_{solar}}{R_{sp}^2} \right) \left(\sum_{i=1}^4 A_i f_i(\mu_i, \nu_i, \phi_i \dots) \right) \quad (1)$$

where C_{sf} is the solar flux at one AU, K_{solar} is the shadow factor, R_{sp} is the Sun-probe distance, A_i ($i = 1, 4$) is the area of each spacecraft component; $f_i(\mu_i, \nu_i, \phi_i \dots)$ is a collective function of specular and diffuse reflectivity coefficients, μ_i and ν_i , illumination angle ϕ_i of

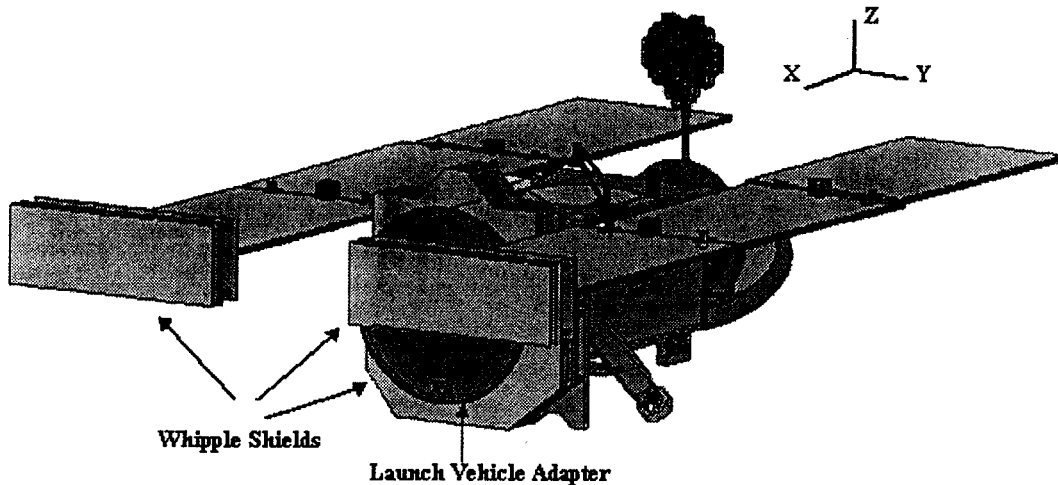


Figure 1: Stardust Structure

each spacecraft component. The effective area for each component is determined from knowledge of the spacecraft orientation (Ref. 3).

The specular coefficient μ_i and diffuse coefficient ν_i , can be expressed in terms of reflectivity coefficient γ_i , diffusivity coefficient β_i , and thermal emissivity coefficient κ_i (Ref. 4, 5, 6):

$$\mu_i = \frac{1}{2}\beta_i\gamma_i \quad (2)$$

$$\nu_i = \frac{1}{3}[\gamma_i(1 - \beta_i) + \kappa_i(1 - \gamma_i)] \quad (3)$$

γ_i is defined as the fraction of total photons reflected from the surface of spacecraft component i , β_i is the fraction of photons reflected specularly (i.e. $\beta_i\gamma_i =$ specularly reflected photons and $(1 - \beta_i)\gamma_i =$ diffusely reflected photons), and κ_i is the parameter which depends on the temperature, emissivity, and accommodation of the spacecraft component i 's surface (for adiabatic surface $\kappa_i = 1$). Here, $i = 1 \dots 4$ are the solar panel, X, Y, and Z plates.

The reconstructed spacecraft attitude information is extracted from the Stardust Telemetry Data System (TDS) and is expressed in terms of quaternions. Currently, the interval between each quaternion data point in the TDS file ranges from a few minutes to several hours. JPL Navigation and Ancillary Information Facility (NAIF) is responsible for post-processing the raw data and delivering the smoothed quaternion product for navigation use.

The refined and improved spacecraft component model was implemented in March 2000. The original spacecraft model was based on pre-launch information (Ref. 7) and uses a simpler flat plate model. Table 1 summarizes the original and updated spacecraft solar radiation model. The improvements over the original model are: (1) updated plate areas

Table 1: ORIGINAL AND UPDATED SPACECRAFT MODEL

Flat Plate	Updated Model	Original Model
Solar Panel		NA
<i>size (m²)</i>	7.97	
<i>specular</i>	0.037	
<i>diffuse</i>	0.264	
X plate		
<i>size (m²)</i>	2.090	2.090
<i>specular</i>	0.100	0.005
<i>diffuse</i>	0.242	0.202
Y plate		NA
<i>size (m²)</i>	2.110	
<i>specular</i>	0.155	
<i>diffuse</i>	0.199	
Z plate		
<i>size (m²)</i>	2.800	10.30
<i>specular</i>	0.122	0.030
<i>diffuse</i>	0.222	0.276

and the associated solar radiation coefficients (i.e., the diffuse and specular reflectivities) (Ref. 8); (2) additional components to represent the detailed structure of the Stardust spacecraft.

Figure 2 shows a comparison plot of the original and updated solar pressure models. As indicated in the figure, the difference in these two models is less than 5%. The accelerations are calculated based on the reconstructed attitude file prior to February 21 and the predicted quaternion file is used afterwards. The acceleration drops during late January are due to the smaller solar radiation effective area as a result of attitude changes for a maneuver.

Small Force

Stardust is designed with an unbalanced thruster configuration which will introduce a ΔV during each attitude control activity. Figure 3 shows the configuration of Stardust's Rocket Engine Modules (REM). Eight 1 - lb thrusters and eight 0.2 - lb thrusters are mounted in four clusters. Each cluster contains two 1 - lb and two 0.2 - lb thrusters. A desired thruster vector can be obtained by combining a specific set of 1 - lb thrusters. The 0.2 - lb thrusters will generate thrust accelerations along spacecraft +Z and $\pm Y$ axes.

The 1 - lb thrusters are mainly used to shape or correct the spacecraft trajectory. It includes Deep Space Maneuver (referred to as DSM) and Trajectory Correction Maneuvers (referred to as TCM). More recently, they also are used during slew maneuvers (i.e. rapidly turn the spacecraft to a specific attitude for optical navigation, DSM, and TCM attitudes ...etc.).

The 0.2 - lb thruster are used in limit duty cycle (LDC) mode and the earlier slews.

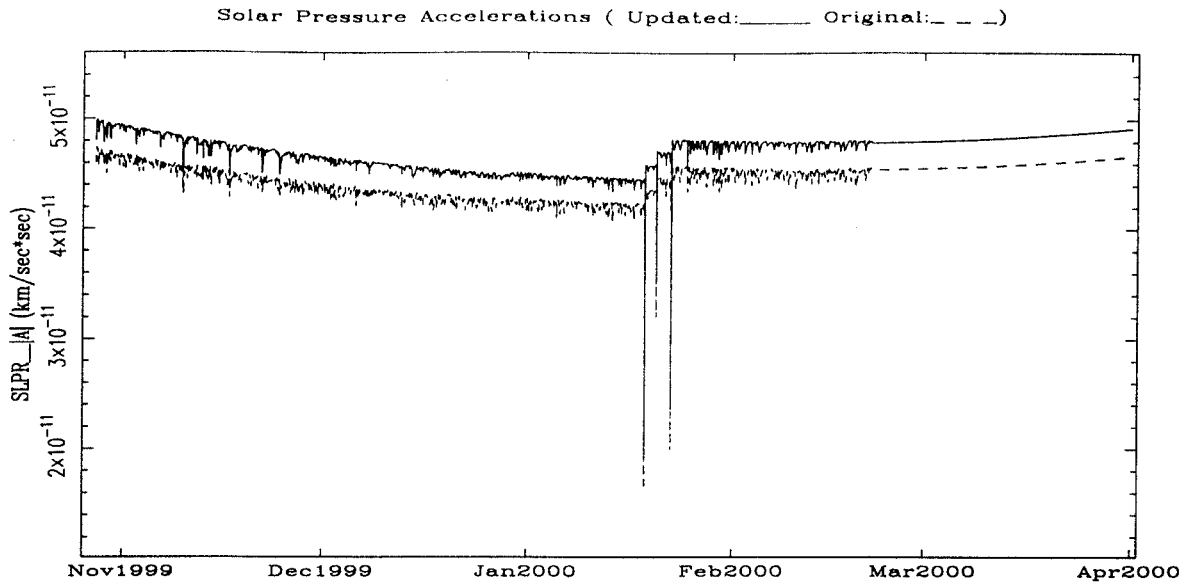


Figure 2: Solar Pressure Acceleration Comparison

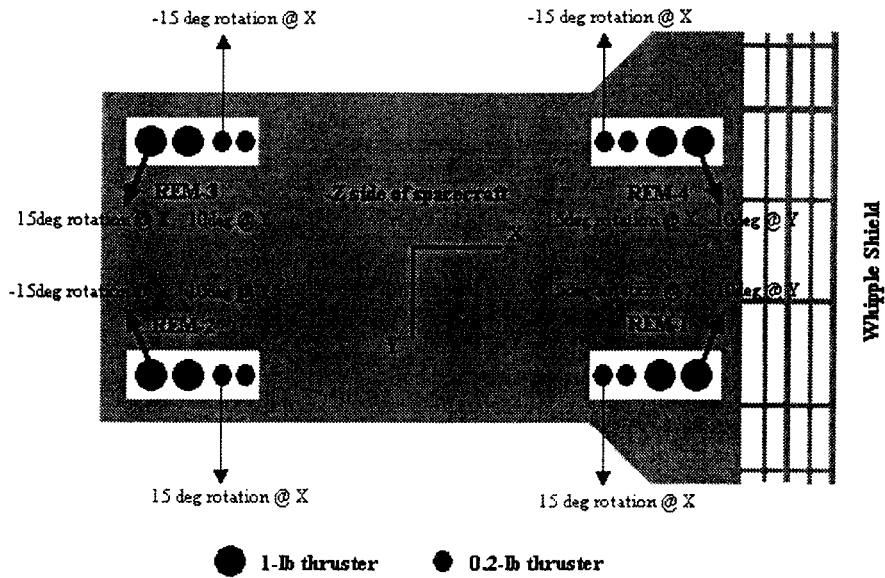


Figure 3: Stardust Thruster Configuration

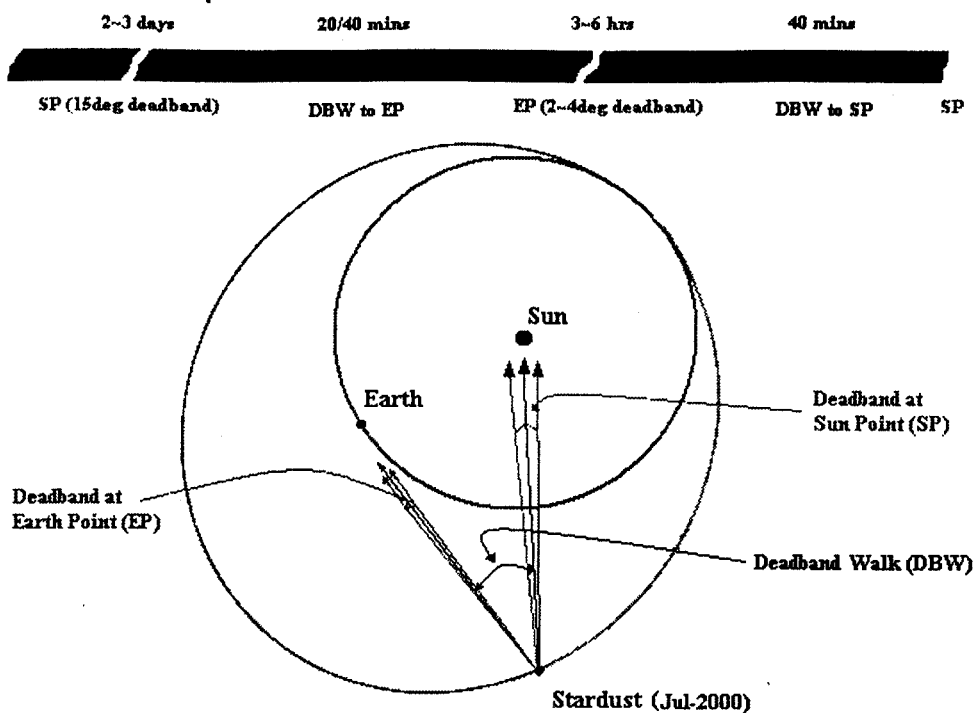


Figure 4: Spacecraft Attitudes during Limit Duty Cycle Mode

LDC is the major attitude control mode and in general, it includes deadband at Sun point, deadband walk from Sun to Earth point, deadband at Earth point, and deadband walk from Earth to Sun point. Typically, during cruise phase deadbands of 15° and 2° to 4° are imposed at Sun point and Earth point respectively (Ref. 9). Figure 4 illustrates the Stardust orientations during limit duty cycle and the associated approximate time duration for each attitude.

Stardust adapts the same file format as Mar Polar Lander (MPL) to model the spacecraft dynamics due to the historical thruster firings (Ref. 10). JPL NAIF Team generates and delivers the reconstructed small force file by extracting and reformatting the information from the small force packets generated by the Stardust on-board algorithm.

The small force packets embedded in the spacecraft telemetry data generally can contain one thruster firing pair or an accumulation of more than one thruster firing pair. Thruster magnitude and orientation information from the accumulated packets are mean values and initially they accounted for the majority of Stardust small force packets. However, for better understanding and characterizing the small force behaviour, the on-change (recording every single thruster event) packets have been used since 29 Mar 2000 and this strategy will continue throughout the entire mission as long as the S/C condition permits.

Recall that the limit duty cycle mode is the primary thruster mode during cruise phase. The 0.2-lb thrusters are used to perform the attitude control in this particular mode. The

Table 2: ON-BOARD SMALL FORCE COMPUTATION

Attitude Mode	Thruster Type	On-Board Calculation Applied
Deadband		
<i>deadband walk</i>	0.2-lb	90% of Primex LDC Eq.†
<i>Sun point</i>	0.2-lb	90% of Primex LDC Eq.†
<i>Earth point</i>	0.2-lb	90% of Primex LDC Eq.†
Slew		
<i>before Y2000</i>	0.2-lb	Primex Pulse Eq.
<i>after Y2000</i>	1.0-lb	Primex Pulse Eq.

†: Jul 99 ~ Sep 00

associated LDC impulse bit (I_{bit} , in $lb-sec$) equation, also known as Primex LDC Equation, for 0.2-lb thrusters can be expressed in terms of tank feed pressure, P_f in psi , and thruster on-time, O_t in sec ($O_t \geq 15msec$) as (Ref. 11)

$$I_{bit} = (3.34 * 10^{-4} * P_f + 2.0 * 10^{-3}) * O_t + 5.3 * 10^{-6} * P_f + 1.56 * 10^{-3} \quad (4)$$

Currently, the on-board flight software for computing the thruster events during the LDC mode is based on the calibrated primex LDC equation. A 0.9 scale factor has been applied to Eq. (4) for on-board small force calculations since July 1999. The on-board formulation for the slews, DSM, and TCM maneuvers is based on the primex pulse mode equation. As mentioned above, the pulse mode records account only for a small portion of the total small force records. The pulse mode equation can be expressed as

$$I_{bit} = (6.11 * 10^{-4} * P_f + 4.39 * 10^{-4}) * O_t + 4.77710^{-3} \quad (5)$$

for the 0.2-lb thrusters, and

$$I_{bit} = (2.723 * 10^{-3} * P_f + 1.29506 * 10^{-1}) * O_t + 2.18210^{-3} \quad (6)$$

for the 1-lb thrusters.

For 0.2-lb thrusters, the pulse mode equation will output 1.85 – 2.04 times more thruster force than the LDC equation. The range is due to the different levels of tank feed pressure and thruster on-time.

Table 2 summarizes the most commonly used attitude modes and the related formulations for reconstructing the small force packets used by the spacecraft flight software.

ERROR SOURCES

The pre-launch acceleration uncertainty (the random part) of attitude control system (ACS) was expected to be $1.5 * 10^{-11} km/s^2$ and no constant bias was anticipated during

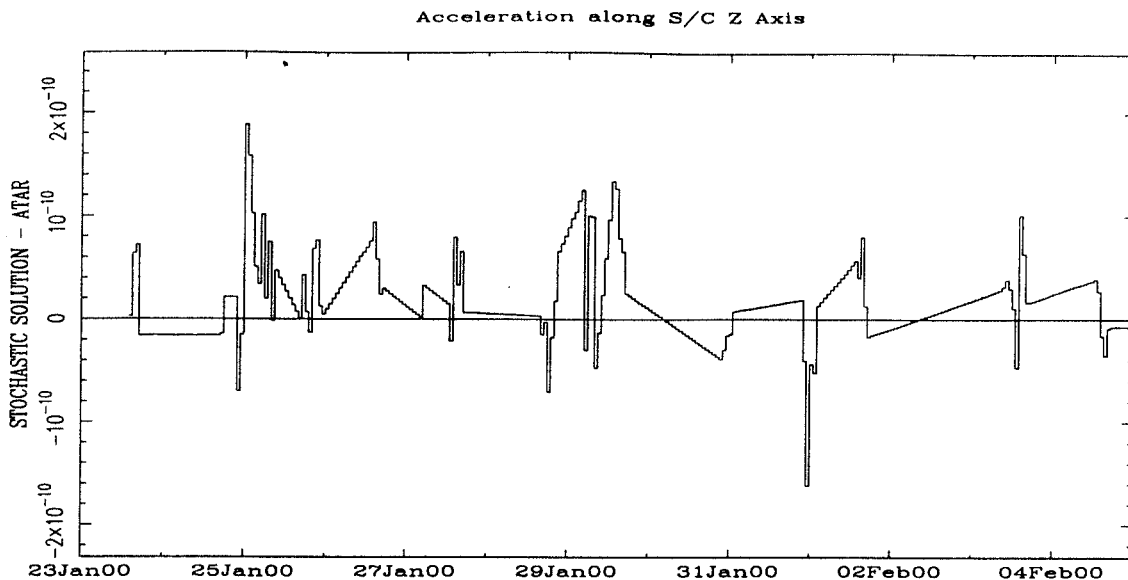


Figure 5: Estimated Stochastic Accelerations

the Stardust cruise phase (Ref. 12). The solar radiation acceleration is roughly in the range of 4.0×10^{-11} at 3 AU to $2.0 \times 10^{-10} km/s^2$ at 1 AU. The uncertainty was expected to be less than 10%.

Stardust Navigation Team (Nav) has been observing stochastic accelerations ranging from 10^{-11} to $10^{-9} km/s^2$ (Ref. 13). A constant acceleration bias of $1.0 - 3.0 \times 10^{-11} km/s^2$ is also detected. Figure 5 shows an example of estimated stochastic accelerations. Clearly it demonstrates an acceleration bias of greater than $2.0 \times 10^{-11} km/sec^2$. The associated predicted two-way Doppler residual is shown on Figure 6. In less than a two-week time span, the predicted residual shows a bias of about 1.5 Hz. The nongravitational spacecraft dynamic models used for the above example are the updated solar radiation model and the on-board generated small forces. The next two sub-sections describe the detailed nongravitational dynamic errors due to the solar pressure and small forces.

Solar Radiation Error

The minimum solar radiation acceleration occurs at late January 2000. At this time, the Stardust orbit is approaching apoapsis and the spacecraft is approximately 3 AU from the Sun. As illustrated in Figure 2, the minimum solar pressure acceleration of the updated model is $\sim 4.5 \times 10^{-11} km/sec^2$. Making a conservative error assumption that 10% of the total solar acceleration contributes to the station line-of-sight direction, the two-way Doppler bias due to the mismodelling is less than 0.3 Hz in a two-week prediction. In reality, the two-way Doppler shift due to the solar radiation error should be much smaller due to:

- the updated solar radiation model being based on more accurate measurements than the original model;

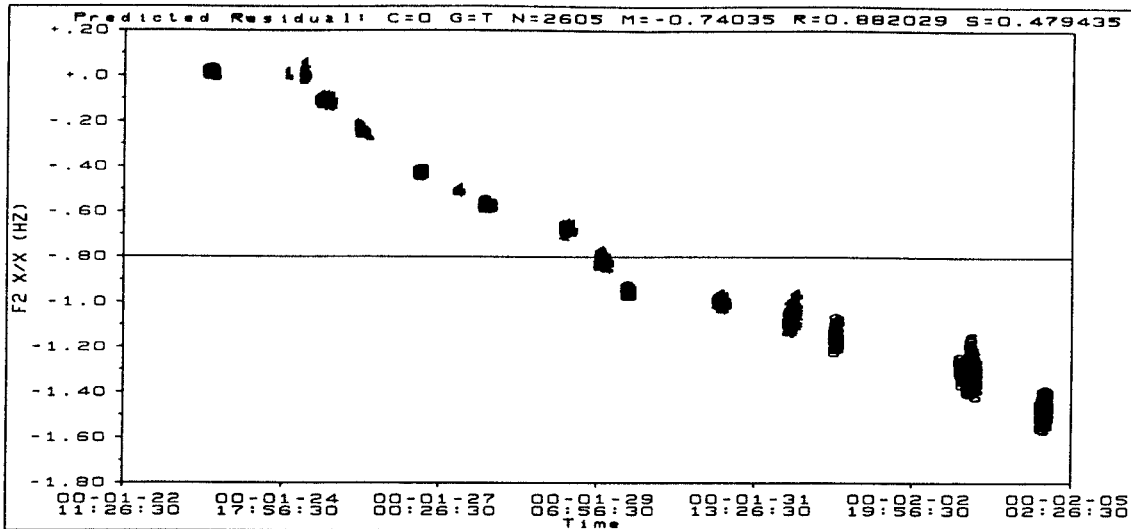


Figure 6: Predicted Two-way Doppler Residual (with On-board generated SMF)

- the estimated solar radiation effective area scale factors having consistently shown less than 5% of corrections in long data arc solutions (apoapsis region);
- the solar pressure error along the station line-of-sight direction being $\cos \theta$ of the total solar radiation error ($\theta = \text{Sun-Probe-Earth angle}$).

Evidently, the predicted Doppler bias observed in Figure 6 is not caused by the solar radiation mismodelling. Furthermore, a large portion of the estimated stochastic accelerations (shown in Figure 5) have much a larger correction than the total solar acceleration (shown in Figure 2). This also strongly suggests that the error source is not from the solar pressure model.

Small Force Error

Several studies (Ref. 10, 14, 15) have demonstrated that in addition to the tank feed pressure and thruster on-times, the thruster off-time since the preceding pulse plays an influential role in affecting the small force computation. The catalyst bed temperature varies exponentially due to the changes of thruster firing frequency or density distribution and it will affect the the thruster output performance. Generally, the thruster off-times during slews are mostly sub-seconds. During deadband walk to Earth point, the off-times are sub-seconds to a few seconds. For the rest of LDC modes, the off-times are usually in the level of seconds, minutes or even hours. Inarguably, the lack of thruster off-times in the I_{bit} equations, Eq. (4), (5), and (6), will result in mismodelling of the on-board small force computations.

Note that at the same level of tank feed pressure and thruster on-time, the pulse mode I_{bit} equation is about 2 times bigger than the LDC mode I_{bit} equation. The on-board

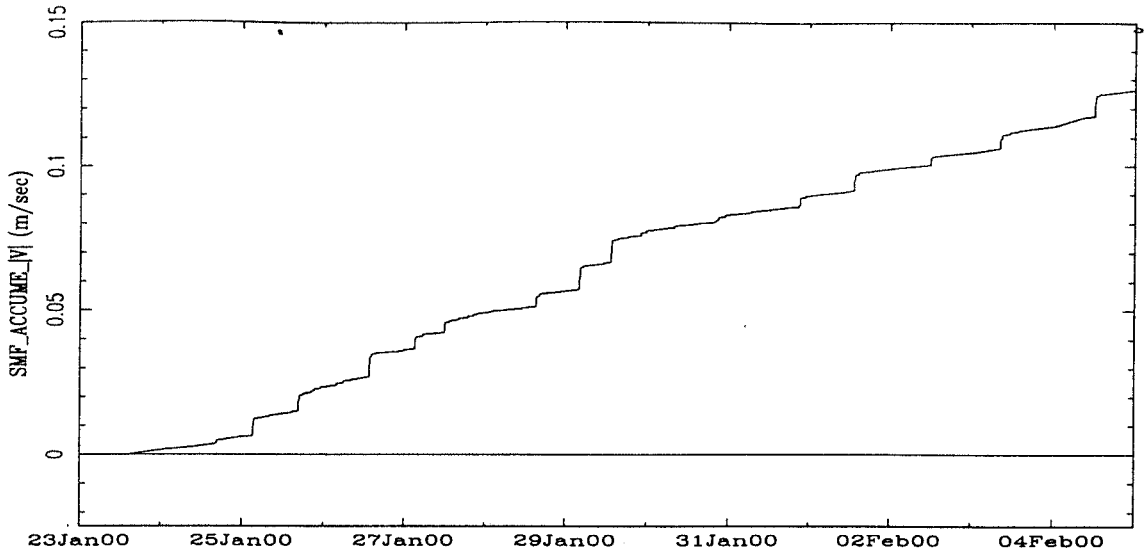


Figure 7: Small Force Cumulated ΔV

algorithm can be pre-set to use one of these equations to reconstruct the thruster Δv . To switch from one mode to the other, a command procedure has to be uploaded in advance. Even if the current flight software can automatically toggle between modes, it still requires the capability of automatically fine tuning the I_{bit} level according the thruster off-time and the revision is not trivial. For a deadband walk or other high frequency thruster activities, the LDC mode equation will underestimate the impulse level significantly. Similarly, for low frequency firings, the LDC mode equation will result in overestimating the impulse level.

Conceivably, the small force mismodelling is the main error source of the spacecraft dynamic models. Further analyses have provided evidence supporting that the small forces are inaccurately modelled:

- the large spikes shown in Figure 5 correspond to the deadband walk to Earth point region which represents the major mismodelling areas;
- applying an overall small force scale factor of ~ 1.2 to the on-board generated SMF will eliminate the Doppler bias in Figure 6;
- a 1.35 (mean value) small force scale factor during the deadband walk to Earth point regions is detected and it easily introduces acceleration errors on the order of $10^{-11} km/sec^2$;

Figure 7 illustrates the cumulated ΔV_i of on-board generated small forces. The summation process is simply done by the following formulation:

$$\Delta V_i = \left| \sum_{i=1}^n \Delta v_i \right| \quad (7)$$

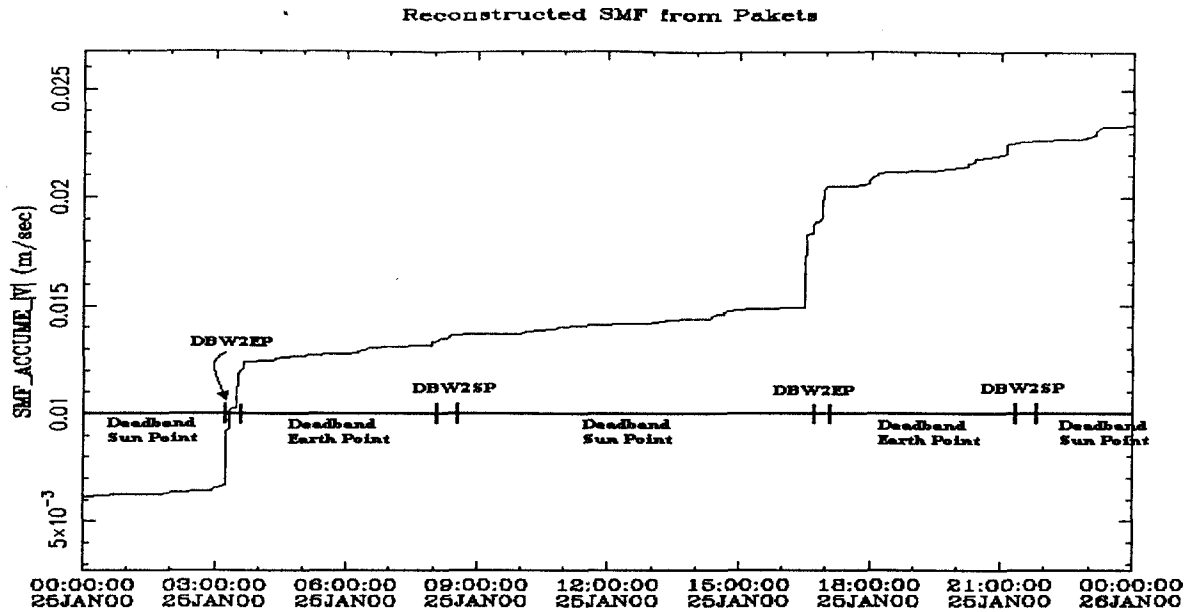


Figure 8: Cumulated Small Forces on 25 Jan 2000

Here, Δv_i is the total delta velocity induced by packet i .

As shown in Figure 7, each of the stair-like step represents the total ΔV needed for the deadband walk from Sun attitude to Earth attitude. Figure 8 shows a more detailed resolution of the attitude changes. As illustrated in Figure 4 and 8, a typical spacecraft attitude change sequence can be summarized as: Sun point (SP) \rightarrow deadband walk to Earth (DBW2EP) \rightarrow Earth point (EP) \rightarrow deadband walk to Sun (DBW2SP). In the above example, it costs about 7 mm/sec to complete a 20-minute DBW2EP.

As a consequence of the small force error analyses, JPL has identified and defined the procedures needed to resolve the spacecraft dynamic mismodellings. Resolutions included:

- requesting LMA to generate small forces information on every event and adapting 40-minute DBW2EP
- developing utility programs to characterize the small force behavior and to analyze and the OD solutions
- constructing a pre-processor for OD filter inputs
- adapting a revised OD strategy to estimate the small force scale factors
- setting up procedures to generate OD updated small forces
- building a calibration process to generate the predicted small forces

The 40-minute DBW2EP strategy has greatly reduced the total ΔV needed to complete a deadband walk with a saving of about 40%. Another benefit of doubling the walk time

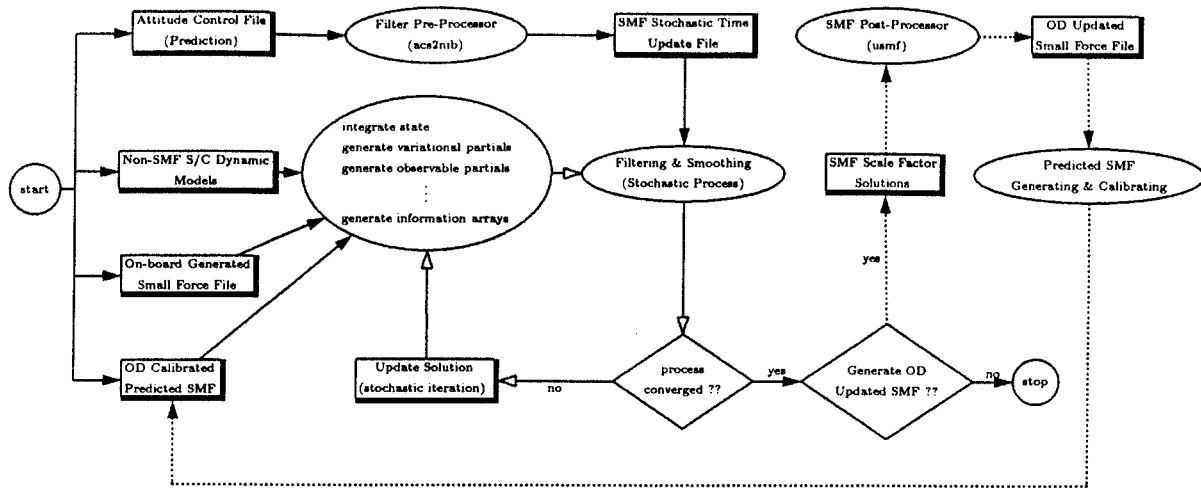


Figure 9: Orbit Determination Flowchart

is to reduce the small force error in this region by about 5%. Although the 40-minute DBW2EP will generate a more accurate predicted orbit because of the smaller total ΔV 's and errors, it still needs a good orbit determination strategy to reconstruct the on-board generated small forces. Numerous tools and utility programs have been built to support the dynamic error analyses, prepare the OD filter inputs, and generate products. The next section describes detailed estimation strategy in dealing with the small force mismodelling.

ORBIT DETERMINATION STRATEGY

The objectives of orbit reconstruction are to determine the spacecraft dynamic mismodellings and to apply the estimation results to improve the propagation models. The mismodelling of small forces is the major contributor to the errors in estimating the orbit and is highly correlated to the thruster firing frequency. Understanding the characteristics of small forces is the key to accurately solve for the small force mismodelling.

Based on pre-launch studies the navigation team assumed that the effect of small forces could be treated by a combination of instantaneous impulsive burns and a stochastic acceleration model. This strategy (conventional filter strategy) depends on using estimates of the small force determined by an on-board algorithm. The technique is perfectly all right if the small force errors fit the random model and the propagation mismodellings are bounded within the uncertainties. However, the above analyses have suggested that the small forces are noticeably mismodelled and the errors are not distributed randomly. The conventional approach is inadequate due to the deficiencies of the on-board algorithm and shortcomings in the strategy such as the lack of *a priori* knowledge of when to apply the impulse burns, indiscriminate aliasing of the dynamic errors, and the difficulty of incorporating the estimation information to enhance the orbit propagation models.

Table 3: ESTIMATED PARAMETERS

Estimated Parameter	A-Priori σ	Remark
Constant Parameters		
<i>epoch state</i>		
<i>position</i>	10^5	<i>km</i>
<i>velocity</i>	10^2	<i>km/sec</i>
<i>solar radiation coefficient</i> [†]		
μ_i	5×10^{-2}	<i>specular</i>
ν_i	2×10^{-2}	<i>diffuse</i>
A_i	$5 \sim 10\%$	<i>% of area (plate)</i>
Stochastic Parameters		
<i>quad. model</i> [‡]		
<i>s/c x</i>	5×10^{-11}	<i>km/sec²</i>
<i>s/c y</i>	5×10^{-11}	<i>km/sec²</i>
<i>s/c z</i>	5×10^{-11}	<i>km/sec²</i>
<i>SMF scale factor</i>		
<i>deadband walk to Earth</i>	0.8	<i>1batch/walk</i>
<i>Earth point</i>	0.3	<i>1batch/2min</i>
<i>deadband walk to Sun</i>	0.3	<i>1batch/walk</i>
<i>Sun point</i>	0.3	<i>1batch/6hours</i>
<i>range bias</i>	100	<i>range unit</i>

†: only solar array and S/C Z plat are estimated

‡: effective only after the end of data arc

In addition to the stochastic acceleration model, the solar radiation biases are estimated as constant parameters and the instantaneous burn parameters often had to be applied where large shifts are observed in the two-way Doppler pass through residuals. The cumbersome conventional filter strategy in reality is not adequate to provide the necessary information to resolve the spacecraft dynamic mismodellings.

A revised filter method has been developed to create a simple and efficient orbit determination strategy. Not only is it specifically designed to deal with Stardust's dynamic mismodellings but the estimation knowledge also can be fed back to optimize the orbit propagation models. Figure 9 demonstrate the orbit determination procedure flowchart.

A key element of the revised estimation strategy is to replace the stochastic acceleration model with a small forces model in which a stochastic scale factor is estimated to correct the error in the onboard small forces. A combination of telemetry data and knowledge of the operations sequence is used to construct the batch times and process noise for a batch sequential filter. The time span for processing the tracking data is decomposed into the relevant LDC attitude modes (ie Sun and Earth pointing phases, the deadband walk from Sun to Earth and the return from Earth to Sun and inertial hold attitudes). A batch sequential filter-smoother is used to process the tracking data with batch times and stochastic process noise determined by the attitude mode. For each batch the filter stochastically estimates a smoothed value of the scale factor to correct the individual (on

Table 4: CONSIDERED PARAMETERS

Consider Parameter	A-Priori σ	Remark
Exp. Gas Leak[‡]		
<i>s/c x</i>	2×10^{-11}	<i>km/sec²</i>
<i>s/c y</i>	2×10^{-11}	<i>km/sec²</i>
<i>s/c z</i>	2×10^{-11}	<i>km/sec²</i>
Troposphere		
<i>dry</i>	1.0	<i>cm</i>
<i>wet</i>	4.0	<i>cm</i>
Ionosphere		
<i>day</i>	75.0	<i>cm</i>
<i>night</i>	15.0	<i>cm</i>
Station Location		
<i>longitude</i>	5×10^{-6}	<i>deg</i>
<i>heightaboveeq.</i>	5×10^{-4}	<i>km</i>
<i>spinaxisdis.</i>	5×10^{-4}	<i>km</i>

[‡]: effective only after the end of data arc

event) small forces ($\Delta V'$ s) computed by the on board algorithm.

Implementation of this filtering strategy entailed incorporating a model for a scale factor to apply to the small forces when integrating the equations of motion and a formulation for the partials of the state with respect to the scale factor for use in estimation of the scale factor. JPL's Orbit Determination Program was modified to include these capabilities. JPL's SIGMA program was used to performing the filtering, smoothing and mapping for estimating the solution.

Estimated and considered parameters for the filter are summarized in Tables 3 and 4. Estimated parameters include the spacecraft state and epoch, solar radiation pressure coefficients and stochastic scale factor and range bias. (Note an apriori uncertainty of 0.3 is assumed for the Sun and Earth pointing phases and for the deadband walk to the Sun., for deadband walk to Earth a 0.8 factor is assumed to account for the greater firing frequency.) To determine the statistics of the solution when mapped to a target, error sources due to exponential gas, station location and media effects are considered in forming the statistics. In addition a stochastic acceleration which is active after the end of the tracking arc is also treated to model the error due to predicted o small forces.

It has been proven that this redesigned filter method is efficient and adequate to deal with the small force mismodelling. The key elements of the revised filter method include: (1) epoch state formulation; (2) estimation of constant solar radiation parameters; (3) estimation of a stochastic small force scale factor; (4) estimation of stochastic two-way range biases; (5) considering parameters for statistic mapping; (6) generating the filter inputs automatically; (7) generating the OD updated small forces based on the stochastic solutions; (8) improving the orbit propagation model significantly by utilizing the estimated

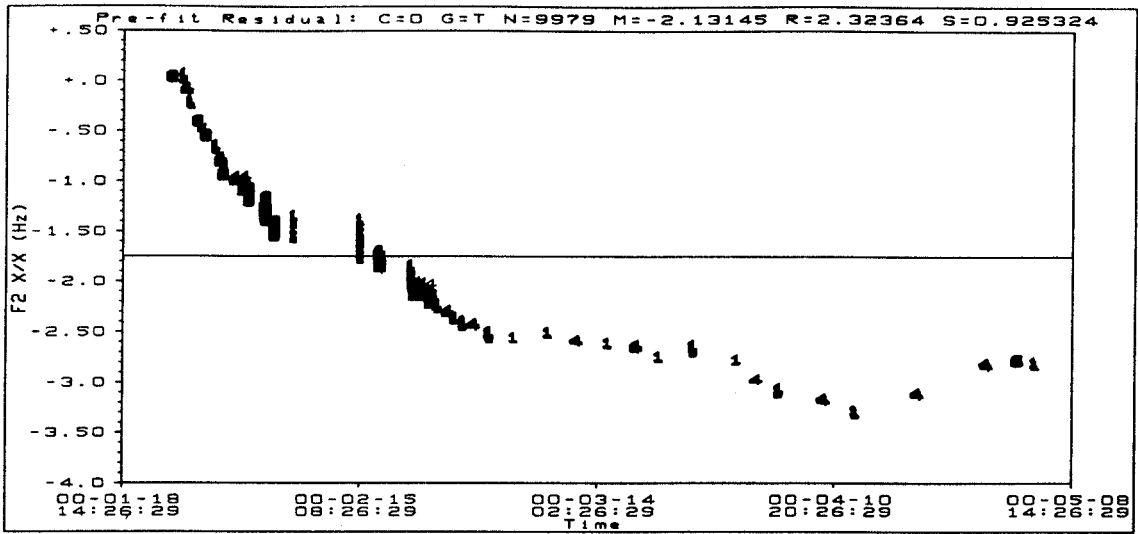


Figure 10: Pre-fit Residual

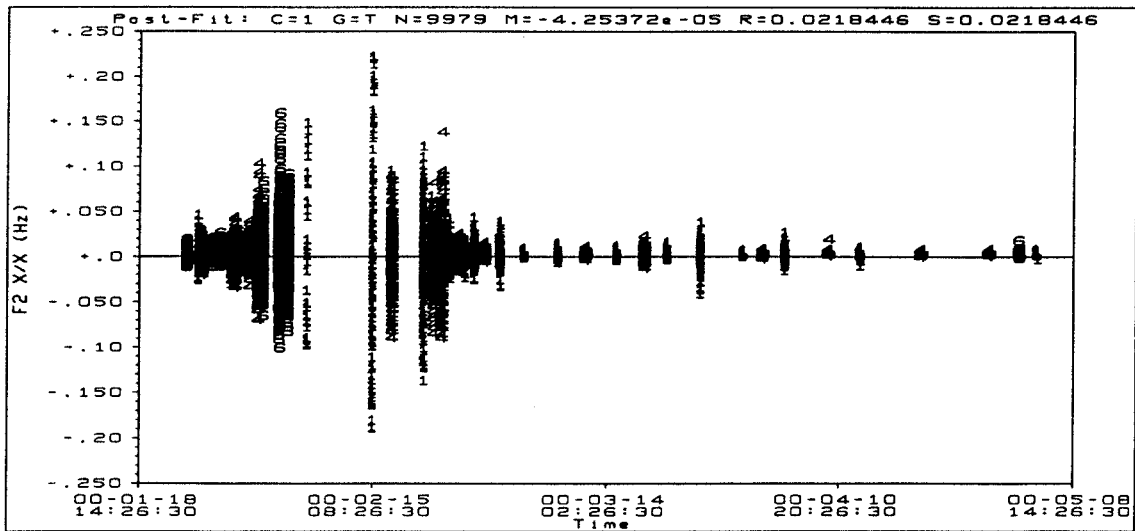


Figure 11: Post-fit Residual

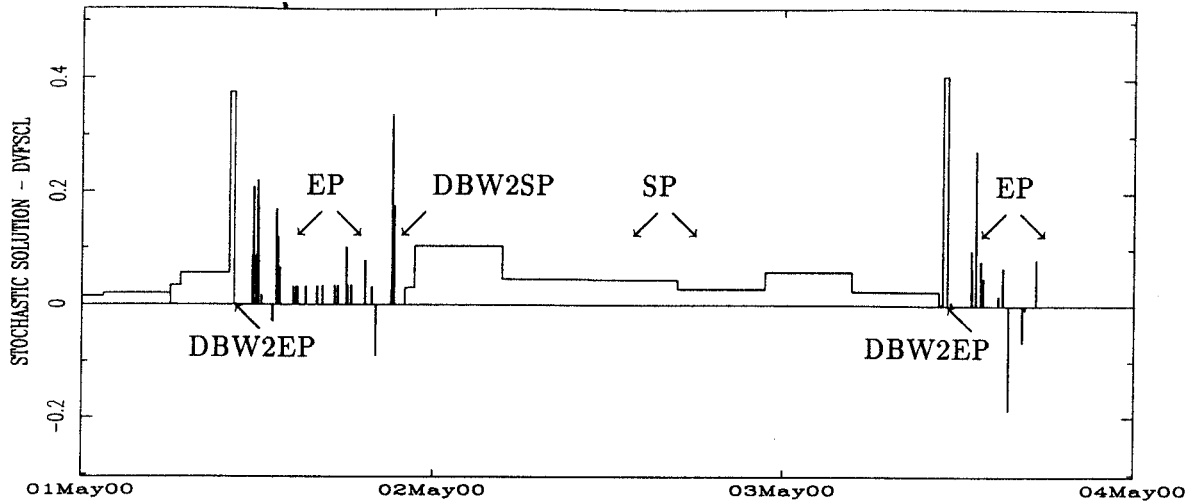


Figure 12: Estimated SMF Corrections

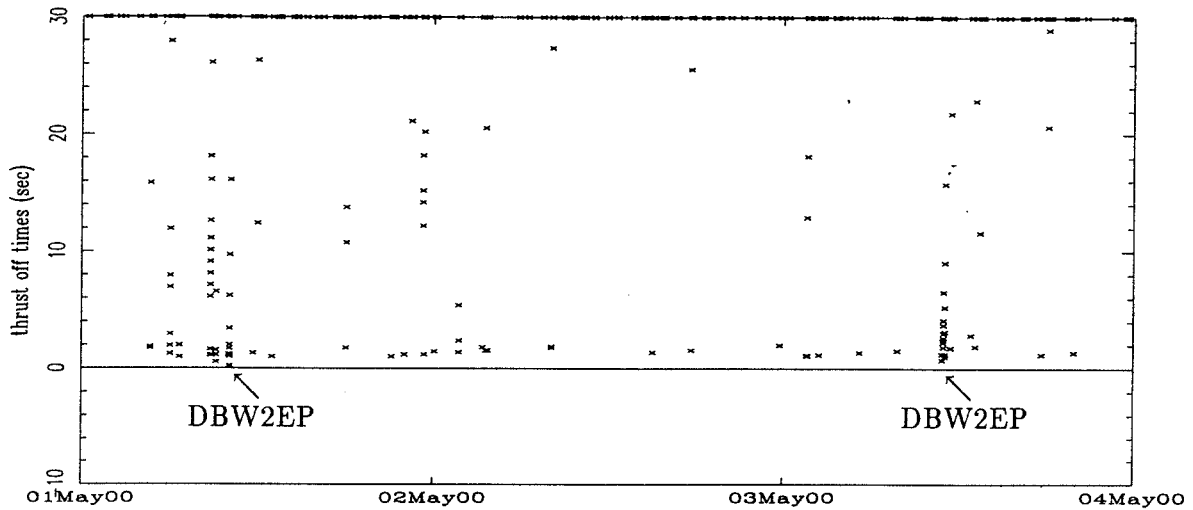


Figure 13: Small Force Thruster Off-time Distribution

knowledge.

RESULTS AND ASSESSMENTS

This section describes the orbit determination results for the reconstructed orbit solution and the assessments of the OD calibrated predicted small forces. The performance of the filter strategy is demonstrated by pre-fit and post-fit Doppler residual figures and the estimated stochastic solutions. Figures of small force comparisons and Doppler predicted residuals are used to evaluate the orbit propagation models.

Figure 10 shows a typical Stardust pre-fit Doppler residual. The spacecraft dynamic models used to generate the trajectory are the updated solar radiation model and the packet

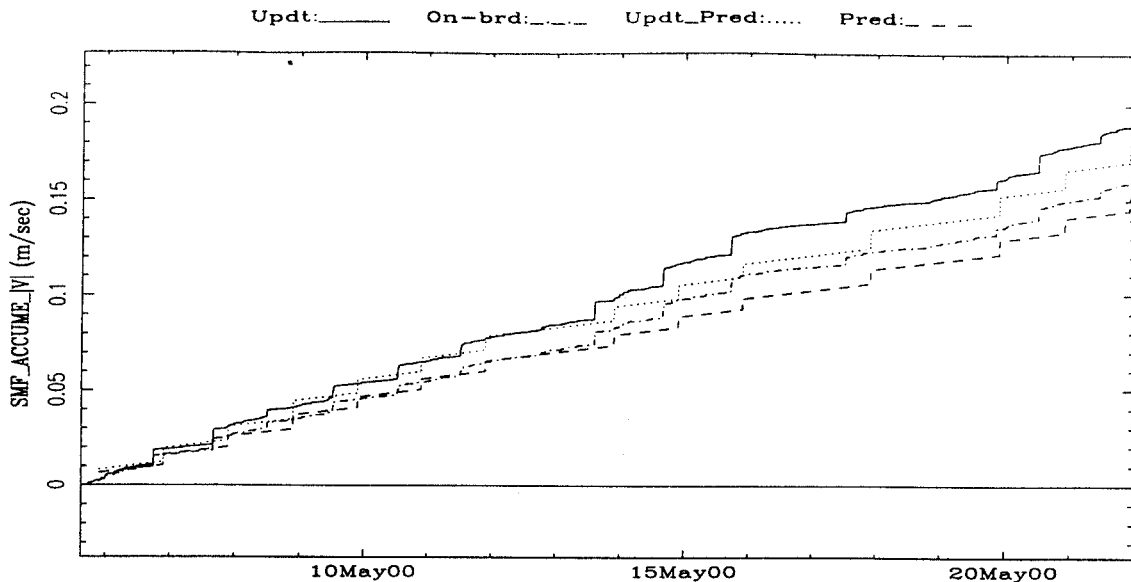


Figure 14: Small Force Comparison

Table 5: SMALL FORCE ERROR SUMMARY

File Type	% Changed from OD Updated SMF (16.5 Days)
Reconstructed Small Force <i>on-board generated</i>	-15.8%
Predicted Small Force <i>OD calibrated</i>	-5.3%
<i>un-calibrated</i>	-20.0%

derived small forces. The Doppler drift caused by the dynamic mismodellings is about 3.0 Hz over a 3-month span. By applying the revised filter strategy, Figure 11 shows the post-fit Doppler residual. The post-fit 1σ data noise is about 0.02 Hz. Due to the solar conjunction, the data noise rises gradually in late January, reaches to a maximum noise level in mid February, and drops back in early March. A deweighting strategy is used in the filtering process to reflect the higher data noise during solar conjunction.

Figure 12 shows a typical example of stochastic small force scale factor solutions. At times the estimated corrections are $\sim 40\%$ more than the on-board generated small forces. The average DBW2EP, EP, and SP corrections are $\sim 39\%$, $\sim 15\%$, and $\sim 10\%$. Figure 13 shows thruster off-time distribution in the same time span with respect to the stochastic solutions in Figure 12. The figure only shows thruster off-times within 30 seconds. The off scaled data points range from half minutes to several hours. As indicated in the figure, the high frequency firings are concentrated in DBW2EP region and they correspond to the two largest corrections shown in Figure 12. These results verify that the small force errors are highly correlated to the thruster off-times.

An OD updated small forces are generated by iterative process which estimates the

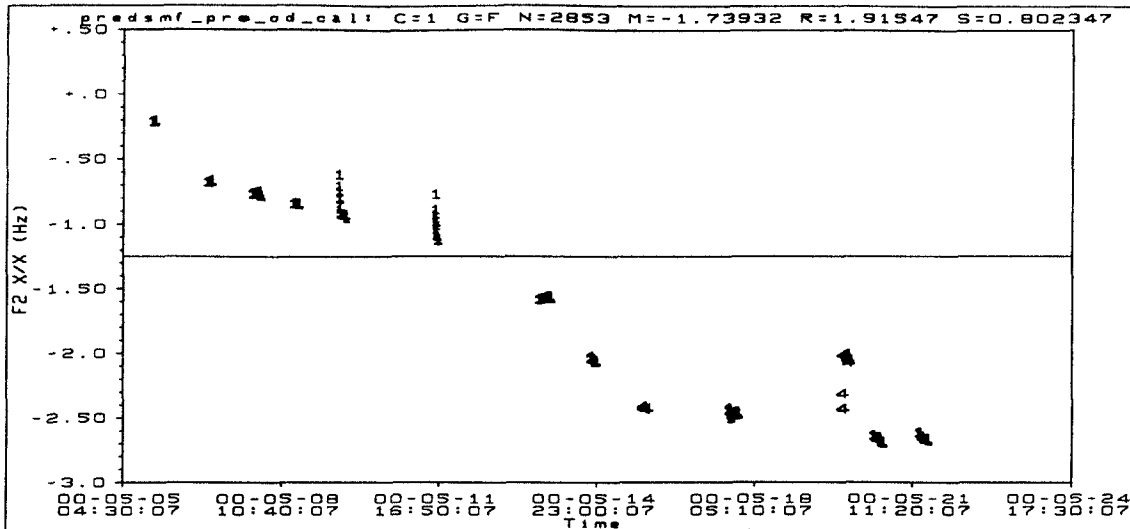


Figure 15: Predicted Residual Without OD Calibrated SMF

trajectory and small forces scale factors that best fit the tracking data and the *a priori* process noise assumptions. The updated small forces estimates, in turn, are used to improve the model for predicting small forces. A detailed description of the procedure for generating the predicted small forces is given in a document by E.Hirst (Ref. 17).

Figure 14 compares the OD-updated small forces (Updt) determined by the stochastic filter with the small forces generated by the on-board algorithm (On-brd). After 17 days the on-board small force is in error by 16%. The figure also compares the predicted small-force models for the same period. This prediction of future small force activity was critical for predicting the Stardust Earth flyby in January 2001 and in planning maneuvers for the flyby, as well as for the comet encounter and Earth return. The predicted models shown in Figure 14 include a model which is derived using parameters from a stochastic scale factor solution generated before the start of this interval (Updt-Pred) and a predicted model based on a pre-launch assessment of the small force activity (Pred). A comparison of the two predicted models with the actual (Updt) model shows a significant improvement in the predicts derived using the small force solutions. The 'Pred' and 'Updt-Pred' show 20% and 5% error with respect to the OD updated small forces over a 17-day time span. Table 5 summarizes the small force errors.

Figures 15 and 16 separately show the Doppler predicted residuals with 'Pred' and 'OD_Cal_Pred' small force models. In this particular example, the trajectory with OD calibrated predicted small force model demonstrates about two times better accuracy than the one with original predicted small force model.

the Stardust spacecraft team members at LMA: Kevin Gilliland, Greg McAllister, Perry Ramsey, Stuart Spath, and Allan Chevront; without their participations and great efforts, it would not have been possible to resolve the small forces anomaly.

REFERENCES

1. "DPTRAJ-ODP User's Reference Manual, Vol. 1", JPL Internal Document, May 1993.
2. Moyer, T.D. "Mathematical Formulation of the Double-Precision Orbit Determination Program (DPODP)", JPL Technical Report: 32-1527, May 1971.
3. Boris V. Semenov, "Stardust Spacecraft Orientation CK File, SDU NAV Version",
4. You, T., J. Ellis, and N. Mottinger, "Navigation of the Space VLBI Mission-HALCA" Paper AAS 98-371, AAS/GSFC 13th International Symposium on Space Flight Dynamics, May 11, 1998
5. Sunseri, R., "Orbit Determination Program Description" Technical Report, JPL, report in progress
6. Georgevic, R., "Mathematical Model of the Solar Radiation Force and Torques Acting on the Components of a Spacecraft" Technical Memorandum 33-494, Jet Propulsion Laboratory, October 1, 1971
7. Nick Smith, "Describes basis for Solar Radiation Pressure Constants", fax, 28 Jun 1996.
8. Perry Ramsey, "Stardust Radiation Parameters", e-mail, 01 Mar 2000.
9. E. Hirst and C. Yen, "Effect of Unbalanced Attitude Control Burns on Stardust Trajectory Design" Paper AIAA/AAS 98-4189, AIAA/AAS Astridynamics Specialist Conference, August 10-12, 1998 / Boston, MA
10. T. McElrath, "Mars Polar Lander (MPL) Small Forces File Modelling Development", JPL IOM 312/00.A-005, 30 Mar 2000.
11. J. Greg McAllister, "Stardust Thruster I-bit Equations", Lockheed Martin interoffice Memo FSMO-00-016, June 24 2000.
12. LMA memo, SD-TM-042.DOC.
13. Prem Menon, "Stardust Small Force Problem Definition", JPL-LMA Weekly Meeting Summary, 24 Feb 2000.
14. G. Mcallister, "Normalized Ibit Vs Offtime - Limit Duty Cycle and slew Data" JPL-LMA weekly meeting presentation, 17 May 2000
15. T. H. You, "OD Analyses during LGA Calibration Slew" JPL IOM 312.C-00-012, 08 Jul 2000
16. "Sigma User's Guide", Version 1.3, JPL Internal Document 10 May 2000.
17. Edward Hirst, "Scale Factor Analysis and Predict Small Forces File Update for TCM-3", JPL Internal Document, Draft, 24 May 2000.